Monatsh Chem
DOI 10.1007/s00706-015-1477-9

ORIGINAL PAPER

Catalytic potentials of homodioxo-bimetallic dihydrazone complexes of uranium and molybdenum in a homogeneous oxidation of alkenes

Mohamed Shaker S. Adam[1,2]

Received: 23 January 2015 / Accepted: 12 April 2015

Abstract The catalytic potentials of dioxomolybdenum(VI) and dioxouranium(VI) homobimetallic bis-ONO tridentate (2-hydroxy-1-benzylidene)malonyl-, succinyl-, and terephthalo-dihydrazone complexes were studied in homogeneous oxidation processes of various aliphatic and cyclic alkenes using aqueous H_2O_2 or TBHP (*tert*-butyl hydroperoxide) as a terminal oxidant. The catalytic potentiality is quantitative and highly selective to afford the corresponding oxide product with $Mo^{VI}O_2$ complexes which is 5 times more than that with $U^{VI}O_2$ complexes using aqueous H_2O_2 or TBHP. Effect of various solvents and temperatures was investigated in the oxidation of 1,2-cyclooctene catalyzed by $Mo^{VI}O_2$ complexes using aqueous H_2O_2 results that the most favored solvent is acetonitrile at an optimal temperature is 70 °C. The mechanistic pathway was tentatively described and discussed.

Graphical abstract

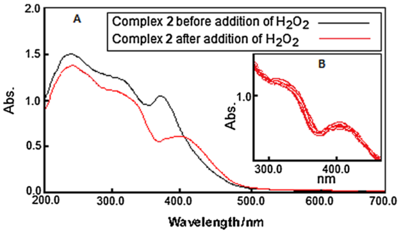

Keywords Dihydrazones · Dioxomolybdenum(VI) · Dioxouranium(VI) · Catalytic oxidation · Alkenes

Introduction

The most important particular application of the catalytic oxidation of alkenes and arenes is the production of industrial chemicals and fine chemicals [1–3]. High attraction on the high-valent molybdenum(VI) complexes is considerable interest in research due to their catalytic activity as internal catalyst [4] for the oxidation of alkenes and arenes. Many transition metal complexes have been reported for oxidation of alkenes [5–10], while dioxomolybdenum Schiff base complexes [4, 11–13] have been of great interest due to their ease and low cost in formation, as well as their sterical and electronical structural features. The catalytic oxidation of alkenes by Mo(VI) complexes has been demonstrated by Mimoun et al. [14]. He suggested that the Mo(VI) complexes form with the oxo reagent intermediates. Those intermediates are responsible for the oxygen transfer in the catalytic processes. Mimoun presented a mechanism, in which the olefin binds to the metal, inserting into the Mo-oxo bond. Subsequent reductive elimination of

---

Electronic supplementary material The online version of this article (doi:10.1007/s00706-015-1477-9) contains supplementary material, which is available to authorized users.

✉ Mohamed Shaker S. Adam
shakeradam61@yahoo.com;
madam@kfu.edu.sa

[1] Department of Chemistry, College of Science, King Faisal University, P.O. Box 380, Al Hufuf 31982, Al Hassa, Saudi Arabia

[2] Department of Chemistry, Faculty of Science, Sohag University, Sohag 82534, Egypt

the resulting metallacycle leads to a metal oxide and the epoxide product. Sharpless et al. [15] suggested an alternative mechanism involving direct transfer of oxygen from the coordinated peroxide to the alkenes.

Consequently, the catalytic activity of MoO_2(VI) catalysts is relevance to the active sites of the majority of molybdo-enzymes [16, 17]. The most valuable types for the active site of several Mo complexes are dioxo complexes of MoO_2(VI) with polydentate nitrogen, sulfur, and oxygen ligands [18–21]. Such active sites are linked to coordinative unsaturation in the MoO_2(VI) complexes catalysts which means coordinatively unsaturated centers. The active sites in MoO_2(VI) complexes may be occupied by labile ligands, i.e. the solvent molecules. This behavior is the major role of a catalytic redox site [22, 23]. MoO_2(VI) complexes have already been shown to be effective catalyst precursors uptake [24–26]. The coordination chemistry of uranium in the form of the uranyl cation species has been largely received considerable attention recently because of their interest coordination chemical behavior, reactivity, and interesting optical, magnetic and catalytic applications, e.g. photocatalysis [27]. The uranyl catalysts not yet find many particular applications mainly in the catalytic activity toward alkenes' epoxidation with various oxidants of high-valent UO_2(VI) complexes [28, 29].

Acyl dihydrazones and their metal complexes have wide applicability, e.g., analytical, medicinal chemistry and biotechnology [30, 31]. Due to their facile keto–enol tautomerization, they have high availability of several potential donor sites can act as multidentate ligands and coordinate with metals of low and high oxidation states [32–35]. At present, significant contributions to literature knowledge regarding the catalytic potentials of homobimetallic complexes have been less explored in the alkene oxidations, especially MoO_2(VI) pattern [36] in combination with multidentate ligands, i.e. dihydrazones, containing bulky fragments in their molecular skeleton. Moghadam et al. [37] reported the catalytic activity of new binuclear molybdenum bis-oxazoline complex in the oxidation of alkenes and sulfides by *tert*-butyl hydrogen peroxide. In the view of those considerations, we developed in this work the complexation of commonly reported multidenate dihydrazone ligands (2-hydroxy-1-benzylidene)malonyl-, succinyl-, and terephthalo-dihydrazone **L1**–**L3** with dioxomolybdenum(VI) and dioxouranium(VI) ions awarding homodioxo-bimetallic complexes **1**–**6** (Scheme 1). The catalytic potentials of those complexes as homogenous catalysts in the oxidation of some various alkenes using either aqueous H_2O_2 or *tert*-butyl hydroperoxide (TBHP) as external oxidants were presented and studied and investigated in various conditions.

Results and discussion

Synthesis and characterization

Synthesis of ligands bis-(2-hydroxy-1-benzylidene)-malonyldihydrazone (**L1**), bis-(2-hydroxy-1-benzylidene)-succinyldihydrazone (**L2**), and bis-(2-hydroxy-1-benzylidene)terephthalodihydrazone (**L3**) is a common method and reported elsewhere [32–35, 38]. Complexation of **L1**–**L3** with either bis(acetylacetonato)dioxomolybdenum or uranyl acetate dehydrate in methanol (1:2) is reported recently by us [26] (Scheme 1). **1**–**6** are characterized by ^{1}H NMR, ^{13}C NMR, and UV–Vis spectra, thermogravimetric analyses (TGA), and elemental analyses (EA). Moreover, they are characterized by IR spectra which are recorded in Table 2.

All complexes **1**–**6** show high air stability in solid phase with decomposition above 300 °C. Ligands in the complexes behaved in a bis-dianionic tridentate manner bonded to the *cis*-MoO_2^{2+} and UO_2^{2+} ions through the phenolic oxygen, the amide oxygen, and Schiff base nitrogen atoms as proved by IR and NMR spectra and previously by X-ray analysis of complex **1** [32]. The X-ray analysis of complex **1** [32] afforded *cis*-MoO_2^{2+} complexes.

In the solid phase, *cis*-MoO_2 complexes **1**, **2**, and **3** are yellow to orange while the UO_2^{2+} complexes **4**, **5**, and **6** are red to brownish red (Table 1). The current complexes are partially soluble in common organic solvents (acetonitrile, acetone, and methanol) but highly dissolved in the coordinated solvents, such as DMSO and DMF.

^{1}H NMR spectra of **L1**–**L3** and complexes **1**–**6** gave conclusive evidence for the complexation mode and the coordinated atoms of **L1**–**L3** to MoO_2^{2+} and UO_2^{2+} ions. The NH and OH resonating signals in **L1** (11.85, 11.47, 11.40, 11.07, and 11.05 ppm, resulted from the diketo-, keto–enol, and dienol forms of **L1**) disappeared completely in the corresponding complexes **1** and **4**. The same behavior was observed in the complexation of **L2** and **L3** with MoO_2^{2+} and UO_2^{2+} ions. The resonating signals of the NH and OH observed at 11.71, 11.70, 11.28, 11.21, 11.17, and 10.13 ppm (due to the tautomeric behavior) in **L2** disappeared in **2** and **5**. In **L3**, the NH and OH proton resonances (11.19, 11.22, and 12.24 ppm) disappeared in **3** and **6** after complexation. These regarding involved that **L1**–**L3** coordinated to the metal ions in the enol form through the phenolic OH group and the dienol OH group. There is a downfield shift of the HC=N resonating proton from 8.28 and/or 8.42 ppm in **L1** to 8.80 and 9.19 ppm in **1** and **4**, respectively, from 8.28 and/or 8.35 ppm in **L2** to 8.77 and 9.14 ppm in **2** and **5**, respectively, and from 8.67 and/or 8.69 ppm in **L3** to 9.00 and 9.32 ppm in **3** and **6**, respectively. This could be due to the coordination of the N

Scheme 1

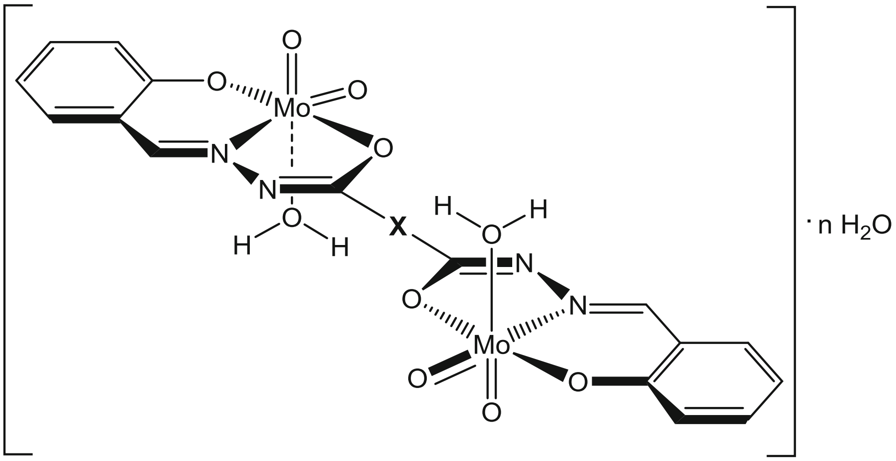

1-3

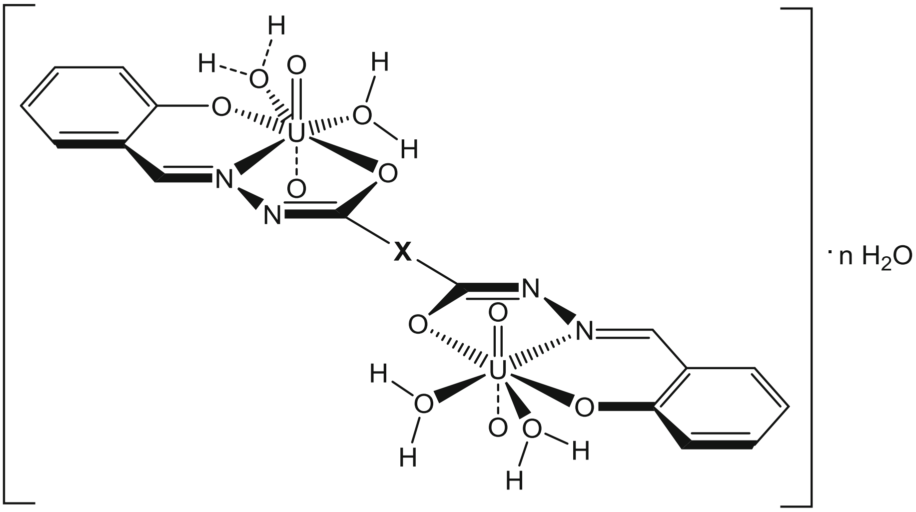

4-6

Complex	X	M (metal ion)	n (crystalline molecules)
1	-CH_2-	Mo^{VI}	1
2	-C_2H_4-	Mo^{VI}	1
3	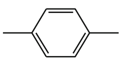	Mo^{VI}	1
4	-CH_2-	U^{VI}	1
5	-C_2H_4-	U^{VI}	0
6	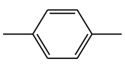	U^{VI}	0

Table 1 Characteristic electronic spectra for the current complexes ([complex] = 1.0 × 10^{-4} mol dm^{-3}) at 298 K

Complex		MW/g mol^{-1}	Electronic spectra (in MeOH)			Color
			λ_{max}/nm	ε_{max}/mol^{-1} cm^{-1}	Assign.	
1	$[(MoO_2)_2L1(H_2O)_2]\cdot H_2O$	646.22	391	33,150	LMCT	Yellow
			338	12,820	*n*–π*	
			251	17,970	π–π*	
2	$[(MoO_2)_2L2(H_2O)_2]\cdot H_2O$	660.25	381	31,900	LMCT	Orange Yellow
			335	18,780	*n*–π*	
			254	17,940	π–π*	
3	$[(MoO_2)_2L3(H_2O)_2]\cdot H_2O$	708.29	404	34,470	LMCT	Orange
			346	12,540	*n*–π*	
			258	17,970	π–π*	
4	$[(UO_2)_2\ L1(H_2O)_2]\cdot 3H_2O$	966.43	392	29,100	LMCT	Brownish Red
			290	16,650	π–π*	
5	$[(UO_2)_2\ L2(H_2O)_2]\cdot 2H_2O$	962.22	395	25,730	LMCT	Brownish Red
			290	18,210	π–π*	
6	$[(UO_2)_2\ L3(H_2O)_2]\cdot 2H_2O$	1010.48	399	29,330	LMCT	Red
			294	14,960	π–π*	

Table 2 Structural significant IR spectral data (KBr, $\bar{\nu}$/cm^{-1}) of the studied ligands **L1–L3** and their corresponding complexes **1–6**

Group	L1	1	4	L2	2	5	L3	3	6
H_2O		3734 w	3734 m br		3736 w	3630 w br		3680 w br	3751 w br
		3440 s br	3434 s br		3438 br	3401 s br		3416 s br	3451 s br
OH	3406 m br			3436 m br			3381 m br		
NH	3264 s br		3218 s br	3207 s br		3226 s br	3208 s br		3213 s br
	3208 s br								
CH aromatic	3058 br		3056 m br	3058 br		3050 m br	3035 br		3067 m br
CH aliphatic	2976 br			2928 br	2927 w br	2925 w br			
C=O	1672 s			1663 s			1643 s		
C=N	1566 s	1617 s	1610 s	1555 s	1615 s	1603 s	1551 m	1608 s	1712 w
	1482 m	1556 m	1545 s	1486 m	1558 m		1487 m	1551 w	1599 m
NCO amide	1374 m	1448 w	1445 w	1406 s	1445 m	1448 w	1365 s	1443 w	1449 w
C–O	1263 s	1337 w	1390 m	1273 m	1329 m	1395 m	1284 m	1333 m	1388 m
N–N	1033 w	1260 w	1298 m	1034 w	1265 m	1303 m	1034 w	1290 m	1298 s
M=O		908 m	905 m		868 m	902 m		921 m	897 m
		813 w	760 w		760 w	762 m		745 w	758 w
M–O phenolic		575 w	599 w		585 w	599 w		618 w	597 w
M–O carbonyl		461 w	483 w		467 w	519 w		463 w	522 w
M–N hydrazone			411 w			409 w			403 w

w week band, *m* medium band, *s* strong band, *br* broad band

atom of the HC=N group (Schiff base group) to the central metal ions. Comparison of the ^{13}C NMR spectra between the free ligands **L1–L3** and their corresponding complexes **1–6** indicates that the **L1–L3** coordinated to the central metal ion in the dienol form. The signal associated with the C=O group (182, 172, and 165 ppm in **L1**, **L2**, and **L3**, respectively) disappeared and new signals appeared after complexation at 167 and 170 ppm in **1** and **4**, respectively, at 173 and 177 ppm in **2** and **5**, respectively, and at 167 and 170 ppm in **3** and **6**, respectively, due to the formation of the C=N group in the dienol from (Scheme 1).

Complexes **1–6** and their corresponding ligands were characterized by IR spectra and are recorded in Table 2. IR spectral data supported that the **L1–L3** formed complexes with either MoO_2^{2+} or UO_2^{2+} within dienol form. Strong vibrational bands at 1672, 1663, and 1663 cm^{-1} assigned to $\nu_{(CO)}$ of the uncoordinated dihydrazones, **L1**, **L2**, and **L3** respectively, disappeared in **1–6**. In **L1**, the assigned band of $\nu_{(C=N)}$ appeared as couple of bands at 1566–1482 cm^{-1}, was shifted to 1617–1556 and 1601–1545 cm^{-1} after coordination to MoO_2^{2+} and UO_2^{2+} ions in **1** and **4**, respectively. Also, in **L2** and **L3**, the same behavior was observed that $\nu_{(C=N)}$ shifted from 1555–1486 to 1551–1487 cm^{-1}, respectively, to 1615–1558 and 1603 cm^{-1} in **2** and **5**, respectively, and to 1608–1551 and 1712–1559 cm^{-1} in **3** and **6,** respectively (Table 2) [28]. According to the tautomeric behavior of **L1–L3** [32–35], the $\nu_{(OH)}$ bands at 3406, 3436, and 3381 cm^{-1} disappeared after complexation with appearance of new bands at the same region as doubled signals (3734–3340, 3736–3438, 3680–3416, 3734–3434, 3630–3401, and 3751–3451 cm^{-1} in **1**, **2**, **3**, **4**, **5**, and **6**, respectively) due to the presence of coordinated water molecules in the complexes [28].

L1–L3 show assigned bands in the UV region only, while their corresponding complexes show remarkable colors in the solution which gives characteristic bands in UV and visible regions (Table 1). Electronic spectra of the complexes have been recorded in methanol at $\approx 1.0 \times 10^{-4}$ mol dm^{-3}. The ligands show bands assigned to intraligand $\pi \rightarrow \pi^*$ and $n \rightarrow \pi^*$ transitions [32–35]. The red shift of the UV bands of **L1–L3** [28] with complexation to 290–296 and 345–356 nm, respectively, proved the complexation of the current ligands to the central metal MoO_2^{2+} and UO_2^{2+} ions. In addition to the intraligand bands in the complexes (290–296 nm), all complexes show new bands at 381–404 nm, assigned to ligand-to-metal charge transfer (LMCT) [28].

Unfortunately, attempts to characterize the complex structure by single crystallography were unsuccessful, despite the crystallographic data of **1** were presented by Zhang et al. [32, 33]. In **1** as cited by Zhang et al. [32, 33], the molybdenum atoms have a distorted octahedral coordination with the donor atoms from the Schiff base tetra-anion and one oxo group occupying the sites of the equatorial planes affording *cis*-MoO_2-units. The other oxo group occupies the apical sites. The remaining apical sites are occupied by water molecules, instead of methanol molecule as remarked elsewhere [32, 33]. The nitrogen atoms of the Schiff base ligands are *trans* to one of the double bonded oxo groups, as observed previously [39].

Recently, similar dihomo diuranyl dihydrazone complex of hydroxylpyridinyl oxalohydazoide has been reported with X-ray crystallographic analyses [40], in which the solvent molecule (DMSO) completed the seven coordination number with a distorted pentagonal bipyramidal geometrical structure.

Thermogravimetric analyses results of complexes **1–6** were evaluated using nitrogen as the gas carrier. The complexes were heated at rate of 10 °C per min from 30 to 600 °C. The thermogram of the studied complexes shows that the complexes decomposed into two successive steps. This attributed to the loss of water molecules in the crystal, coordinated water molecules in the complexes for the first and second steps, respectively (Supplementary Material). TGA data confirmed the tentative molecular structure of the recent complexes **1–6**.

In the thermogram of the complexes, the first endothermic weight loss of **1** was observed between 100 and 120 °C with mass loss value ($\Delta m_{rel} = 2.19$ %) approximately agreeing with the expected one ($\Delta m_{rel} = 2.78$ %) and ascribed to the loss of one water molecule. This suggests that the water molecule was part of the lattice structure in complex **1**. Similar behavior for complexes **2** and **3**, the first endothermic weight loss was observed in the same temperature range with mass loss values ($\Delta m_{rel} = 2.11$ and 2.04 %) approximately agrees with the expected one ($\Delta m_{rel} = 2.72$ and 2.54 %) for **2** and **3**, respectively, suggesting that both **2** and **3** have one water molecule in crystal lattice. Also in complex **4**, the loss of the crystalline water molecule detected in the same area with experimental mass loss value ($\Delta m_{rel} = 1.57$ %) agrees with the calculated mass loss ($\Delta m_{rel} = 1.86$ %). Complexes **5** and **6** did not show any weight loss at the range from 180 to 230 °C (Supplementary Materials). This means that the crystal lattice of complexes **5** and **6** probably does not have any water molecules (Scheme 1). In complexes **1–3**, the two coordinated water molecules were lost at 180–230 °C with an observed mass loss value ($\Delta m_{rel} = 5.33$, 5.24, and 5.01 %) which agrees with the expected value ($\Delta m_{rel} = 5.73$, 5.57, and 5.21 % for **1**, **2**, and **3**, respectively).

The decomposition losses ($\Delta m_{rel} = 7.27$, 7.05, and 6.91 %) occurred at the range 180–230 °C agree with the theoretical $\Delta m_{rel} = 7.59$, 7.48, and 7.12 %, respectively, to complexes **4**, **5**, and **6**. This is due to the loss of the four coordinated water molecules to the two central UO_2^{2+} ions. The TGA results support that the two homo-uranyl ions in each complex molecule of **4**, **5**, and **6** have seven coordination number to the bis-dihydrazone ligand and water molecules (Scheme 1).

All complexes **1–6** decomposed without melting above 300 °C.

Catalytic activity

The catalytic performance of *cis*-MoO_2- and UO_2 complexes **1–6** was investigated in the oxidation of some aliphatic and cyclic alkenes with aqueous H_2O_2 and *tert*-butyl hydroperoxide (TBHP) as oxygen donors. A series of

Table 3 Oxidation yield (1,2-epoxycyclooctane) of 1,2-cyclooctene catalyzed by **1–6** using aqueous H_2O_2 in acetonitrile

Entry	Complex	Conversion/%[a]		Selectivity product yield/%[b]		Reactant residue/%		TON[c]		TOF[d]	
		H_2O_2	TBHP	H_2O_2	TBHP	H_2O_2	TBHP	H_2O_2	TBHP	H_2O_2	TBHP
1	**1**	95	97	89	93	5	4	89	93	11.12	46.50
2	**2**	97	99	95	96	3	2	95	96	11.87	48.0
3	**3**	96	98	93	94	4	2	93	94	11.62	47.0
4	**4**	48	53	20	23	52	47	20	23	2.50	11.50
5	**5**	53	56	25	25	47	44	25	25	3.12	12.50
6	**6**	49	54	17	19	51	46	17	19	2.12	9.50

[a] The reaction of 1,2-cyclooctene (1.0 mmol) and complexes **1–6** (0.01 mmol) with aqueous H_2O_2 (4.16 mmol) in 10 cm^3 acetonitrile at 70 °C for 8 h or TBHP (2.0 mmol) at 70 °C for 2 h

[b] The yield percentage of the target oxide product (1,2-epoxycyclooctene) based on GC results

[c] TON (turnover number) = ratio of moles of product (here is the obtained oxide) to the moles of catalyst

[d] The corresponding TOF (turnover frequency) (TON/h) values are shown in parentheses [mol (mol catalyst)$^{-1}$ h^{-1}]

blank experiments revealed that the presence of both catalyst and oxidant is essential for an effective catalytic oxidation *cis*-1,2-cyclooctene (Table 3). To find the suitable reaction conditions, the effect of various reaction parameters that may affect the chemo- and stereoselective conversion was studied. Type and concentration of catalysts, nature and concentration of oxidants, solvent, and temperature are the factors that have been evaluated to optimize the catalytic processes.

Catalyst complexes effect

To evaluate the catalytic activity of complexes **1–6**, oxidation of *cis*-1,2-cyclooctene as a model substrate in acetonitrile catalyzed **1–6** (0.01 mmol) has been investigated using either aqueous H_2O_2 (4.16 mmol) at 70 °C for 8 h or TBHP (2 mmol) at 70 °C for 2 h as the oxygen source. The oxide product (1,2-epoxycyclooctene) thus obtained was analyzed by GC. Control experiments showed that no epoxide was formed in a measurable extent in the absence of any catalyst. All experimental results obtained were collected in Table 3. The controlled catalytic processes using **1–6** were entirely chemo- and stereoselective for oxidation. 1,2-Epoxycyclooctene as the only product was obtained in highest scale but in some cases it was found some other side products in various conditions as recorded by the turnover numbers and turnover frequencies (Table 3), especially with catalysts **4**, **5**, and **6**.

cis-MoO_2 complexes **1–3** afforded high catalytic control and chemoselectivity for the conversion of 1,2-cyclooctene using either aqueous H_2O_2 or TBHP as a terminal oxidant. Table 3 presents excellent conversion percentage (89, 95, and 93 % with H_2O_2 and 93, 96, and 94 % with TBHP using **1**, **2**, or **3**, respectively (Table 3, entries 1–3).

The uranyl units **4**, **5**, and **6** attain low conversion and control selectivity in the same conditions (20, 25, and 17 % with H_2O_2 and 23, 25, and 19 % with TBHP using **4**, **5**, or **6**, respectively) with remaining high amount of the reactant in the reaction media and some other unknown side products, as observed by GC (Table 3, entries 4–6). UO_2 complexes **4–6** afforded low catalytic potential compared to *cis*-MoO_2 complexes **1–3**. Consequently, the catalytic potentiality of 1,2-cyclooctene oxidation is quantitative and highly selective to the corresponding oxide product with *cis*-MoO_2 complexes **1–3** which is 5 times more than that with $U^{VI}O_2$ complexes **4–6** using either aqueous H_2O_2 or TBHP as terminal oxidant in the same conditions. UO_2 complexes are found to serve many catalytic processes as active catalysts, e.g. thermal oxidation of CO, NO, and volatile organic compounds [41, 42]. Nevertheless, UO_2 complex catalysts are yet to find many practical applications, mainly because of their inherent natural radioactivity [29, 43]. From TGA data, the two particular coordinated water molecules complete the coordination number seven of the UO_2 complexes, c.f. Scheme 1, compared to similar reported UO_2 complexes [40]. According to the less crystallographic data of **4–6**, the most common geometry of the ligand around the two uranyl atoms is close to pentagonal bipyramidal with the axial O=U=O moiety, as reported before [40, 44, 45]. Probably, the three donor atoms of the ligand N, O, and O with the two coordinated water molecules may be in the equatorial position. This tentative geometrical structure of **4–6** may support the reason of their low catalytic potential toward oxidation of alkenes with either aqueous H_2O_2 or TBHP as oxygen source.

Oxidant effect

The catalytic potential toward oxidation of 1,2-cyclooctene with either aqueous H_2O_2 or TBHP as oxygen

Table 4 Oxidation yield product of some alkenes catalyzed by **1**, **2**, or **3** using aqueous H_2O_2

Entry	Alkene	Product[a]	Conversion product yield /%[b], selectivity /%			Time /h
			1	**2**	**3**	
1	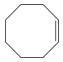	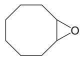	95 (89)	97 (93)	96 (93)	8
2	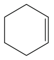	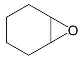	90 (86)	92 (89)	92 (89)	8
3	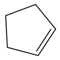	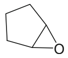	85 (91)	87 (90)	89 (92)	8
4	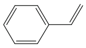	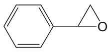	79 (42)	81 (44)	83 (45)	9
5	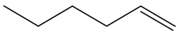	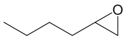	73 (68)	77 (71)	80 (75)	10
6	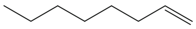	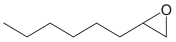	62 (56)	64 (57)	67 (61)	10.5
7	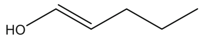	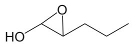	66 (55)	64 (54)	65 (57)	10

[a] Reaction of alkene (1.0 mmol) with aqueous H_2O_2 (4.16 mmol), catalyzed by complexes **1**, **3**, or **5** (0.01 mmol) in 10 cm^3 acetonitrile at 70 °C

[b] The yield based on GC results and conversion percentage (selectivity percentage)

source catalyzed by complexes **1–3** is presented in Table 3. The obtained results from Table 3 assumed that the catalytic processes with TBHP are highly successful than those with aqueous H_2O_2.

Aqueous H_2O_2 as terminal green oxidant is less effective in alkenes oxidation compared to the organic peroxides, i.e. TBHP, as reported in the literatures [46–49]. Particularly, oxidation processes of some aliphatic and cyclic alkenes catalyzed by either **1**, **2**, or **3** and oxidized by aqueous H_2O_2 afforded high potential and chemoselectivity compared to those with TBHP (Tables 3, 4, 5). Oxidation processes with aqueous H_2O_2 consumed longer time (8–10.5 h) compared to TBHP (2–3.5 h) in the same conditions (molar ratio of substrate:catalyst = 100:1). The excess required amount of aqueous H_2O_2 (4.16 mmol, Table 4) compared to that of TBHP (2.0 mmol, Table 5) was resulted either from its decomposition in the presence of the *cis*-MoO_2 complex [50] or the presence of high amount of water [28]. The high amount of water in aqueous H_2O_2 (30 % mol percentage of H_2O_2) may play a major for the catalytic potentiality, which reduced the reactivity of aqueous H_2O_2 as an oxygen source compared to TBHP with low amount of water. Furthermore, the organic nature of TBHP in the organic solvent, e.g. acetonitrile, may improve its reactivity compared to aqueous H_2O_2 [49].

The catalyst/substrate molar ratios

The effect of the catalyst was discovered by insertion of different molar ratios of the complex catalysts **1–3** to 1,2-cyclooctene in the oxidation process (0.01, 0.02, or 0.04:1, respectively) using aqueous H_2O_2 in acetonitrile at 70 °C for 8 h. The results are reported in Table 6 and presented in Fig. 1a. The increase of the catalyst molar ratio to two double amounts improved the rate of 1,2-cyclooctene oxidation affording good yield of conversion after 4–5 h of the running processes (Table 6, entries 4 and 5; 77, 84, and 62 % with 0.01, 0.02, and 0.04 mmol of **1**, respectively). Similar behavior took place for catalysts **2** and **3**. After 4 h of the 1,2-cyclooctene oxidation with catalyst **2**, the control conversion reached to the highest values using 0.02 and 0.04 mmol afford 90 and 72 %, respectively (entries 3 and 4). With catalyst **3**, the conversion afforded 85 and 75 % of the yield product after 4 and 3 h using 0.02 and 0.04 mmol of **3**, respectively (entries 3 and 4). But by running the time with the two double amounts of catalysts (0.02 and 0.04 mmol, entries 5 and 6), the control chemo- and stereoselectivity reduced to afford lower yield with enhancing of other side unknown products (controlled by GC). After long time (ca. 10–12 h), the 1,2-cyclooctene oxidation using 0.02 or 0.04 mmol of catalyst **1**, **2**, or **3**, showed that the control conversion of 1,2-

Table 5 Oxidation yield product of some alkenes catalyzed by **1**, **2**, or **3** with TBHP

Entry	Alkene	Product[a]	Conversion product yield /%[b], selectivity /%			Time, h
			1	**2**	**3**	
1	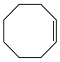	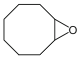	97 (93)	99 (96)	98 (94)	2
2	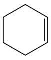	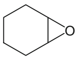	96 (94)	97 (96)	99 (97)	2
3	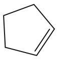	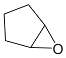	93 (88)	96 (92)	96 (93)	2
4	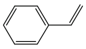	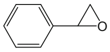	68 (83)	65 (87)	71 (88)	2.5
5	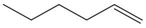	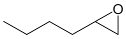	77 (67)	82 (75)	82 (73)	3
6	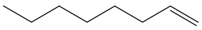	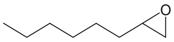	74 (63)	73 (65)	77 (64)	2.5
7	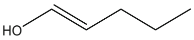	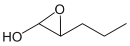	69 (59)	67 (58)	71 (59)	3.5

[a] Reaction of alkene (1.0 mmol) with TBHP (2 mmol), complexes **1**, **3**, or **5** (0.01 mmol) in 10 cm^3 acetonitrile at 70 °C

[b] The yield based on GC results and conversion percentage (selectivity percentage)

Table 6 The time dependence of the product percentage of 1,2-cyclooctene oxidation catalyzed by **1**, **2**, or **3** with different amounts of oxidant (molar ratios) aqueous H_2O_2

Entry	Time/h	Oxidation product of 1,2-epoxycyclooctene yield/% (selectivity)[a,b]								
		1			**2**			**3**		
		0.01	0.02	0.04	0.01	0.02	0.04	0.01	0.02	0.04
1	1	18	21	27	32	36	38	22	25	26
2	2	41	44	46	58	65	67	43	50	53
3	3	57	61	63	74	86	72	69	72	75
4	4	68	70	62	81	90	70	77	85	72
5	5	77	84	58	88	82	61	85		70
6	6	80	82	52	89	80		88	89	
7	7	85	79		92	80	55	90		67
8	8	89	78	47	95	79	54	93	86	65
9	10	89	77		95	78		93	83	
10	12	89	74	44	95	76	50	93		62
Slope[c]		19.4	20.5	20.8						

[a] Reaction of 1,2-cyclooctene (1.0 mmol) with aqueous H_2O_2 (4.16 mmol), complexes **1**, **3**, or **5** in 10 cm^3 acetonitrile at 70 °C to give the maximum yield of the oxide product

[b] The yield based on GC results and selectivity percentage

[c] The slope is a deduced value for the first 3 h of the rate of oxidation conversion of 1,2-cyclooctene reaction

cyclooctane reduced to the lowest amounts, especially with 0.04 mmol of **1**, **2**, or **3** to afford 44, 50, and 62 % of the control product, respectively (Table 6, entries 9 and 10). On the other hand, using the low mount of the catalyst (0.01 mmol of **1**, **2**, or **3**) in the 1,2-cyclooctene oxidation with aqueous H_2O_2 in acetonitrile after 8 h at 70 °C is highly control chemo- and stereoselective to the target oxide product (Table 6, entry 8) awarding 89, 95, and 93 % yield of the oxide product with **1**, **2**, or **3**, respectively, with unremarkable amount of the reactant in the reaction media, as recorded by GC (ca. 2–5 %), cf. Table 3.

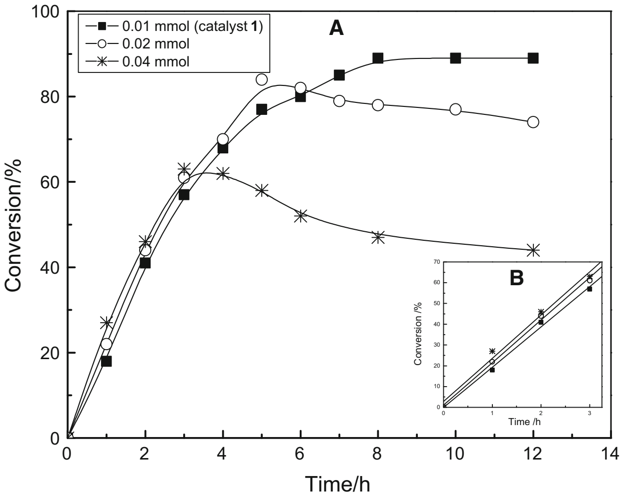

Fig. 1 **a** The time dependence of the conversion percentage of 1,2-cyclooctene catalyzed by **1** in various ratios (0.01, 0.02, or 0.04 mmol) with aqueous H_2O_2 as a terminal oxidant. **b** The time dependence of the conversion percentage of 1,2-cyclooctene catalyzed by **1** in various ratios (0.01, 0.02, or 0.04 mmol) with aqueous H_2O_2 as a terminal oxidant for the first 3 h

Although the increase of the catalyst complexes of the MoO_2^{2+} unit amounts (from 0.01 to 0.02 and 0.04 mmol) enhanced the reaction rate and the catalysts' reactivity, it did not improve the control chemo- and stereoselectivity of conversion. It increased the further 1,2-cyclooctene oxidation to other side unknown products (observed by GC) (Fig. 1a), as observed previously [51, 52]. The slope of the conversion rate of 1,2-cyclooctene oxidation with aqueous H_2O_2 catalyzed by **1** for the first 3 h could be deduced from Fig. 1b and recorded in Table 6. The observed rate constant values indicate that the rate of oxidation within highest amount of catalyst complex **1** (0.04 mmol) is faster than that within the lower amounts (0.01 and 0.02 mmol) of the catalyst. This may be attributed to the catalytic potential of the studied complex catalysts.

Solvent effect

The catalytic potential of some transition metal complex catalysts has been remarkably impacted by the nature of the solvent on the alkene oxidation which was studied recently with different oxidants [49, 52–54]. The influence of different solvents, i.e. acetonitrile, methanol, acetone, tetrahydrofuran (THF), dichloromethane, and chloroform, on the oxidation of 1,2-cyclooctene catalyzed by complexes **1**, **2**, or **3** with either aqueous H_2O_2 or TBHP as the oxygen donor at 70 °C was investigated.

The results in Table 7 illustrate the conversion control and chemoselectivity of 1,2-cyclooctene in the presence of either aqueous H_2O_2 or TBHP with a catalytic amount of *cis*-MoO_2 complexes **1**, **2**, or **3** (0.01 mmol) in different solvents. The trend of the observed solvent effect was ordered as: acetonitrile > chloroform > dichloromethane > methanol > acetone > THF. The highest conversion percentages were obtained in acetonitrile (89, 95, and 93 % with aqueous H_2O_2 after 8 h and 93, 96, and 94 % with TBHP after 2 h, catalyzed by **1**, **2**, and **3**, respectively).

It seems that in aprotic solvents, i.e. acetonitrile, and in lowest dielectric constants, i.e. chloroform and dichloromethane, a high oxidation conversion is observed using catalyst complexes **1**, **2**, or **3**. These results were consistent with those previous results published by Rayati et al. [52] in the investigated catalytic activities of vanadium(IV) Schiff base complexes in the 1,2-cyclooctene epoxidation reaction with TBHP and also by Grivani et al. [51].

In methanol, the conversion control percentages with either aqueous H_2O_2 or TBHP were moderate compared to the results obtained in acetonitrile (Table 7, 49, 39 and 48 % with aqueous H_2O_2 and 43, 45, and 51 % with TBHP, catalyzed by **1**, **2**, and **3**, respectively). As seen from Scheme 2 (II), the presence of unoccupied coordination sites on the metal center (Mo) of the catalyst is crucial for its catalytic performance [1]. Therefore, with aqueous H_2O_2 or TBHP, methanol is of smaller size

Table 7 Oxidation yield product (1,2-epoxycyclooctane) of 1,2-cyclooctene catalyzed by **1**, **2**, or **3** with aqueous H_2O_2 or TBHP in different solvents

Solvent[a]	Acetonitrile		Methanol		Acetone		THF		CH_2Cl_2		$CHCl_3$	
	H_2O_2[b]	TBHP[c]	H_2O_2	TBHP	H_2O_2	TBHP	H_2O_2	TBHP	H_2O_2	TBHP	H_2O_2	TBHP
Oxidation product yield/%												
1	89	93	49	43	15	37	26	27	9	45	16	56
2	95	96	39	45	18	45	17	22	9	46	13	57
3	93	94	48	51	13	42	27	27	4	53	23	59

[a] The reaction of 1,2-cyclooctene (1.0 mmol) with aqueous H_2O_2 (4.16 mmol) or with TBHP (2.0 mmol) catalyzed by **1**, **3**, and **5** (0.01 mmol) in 10 cm^3 solvent at 70 °C

[b] The percentage of the oxide product (selectivity) obtained by GC using aqueous H_2O_2 as terminal oxidant after 8 h

[c] The percentage of the oxide product (selectivity) obtained by GC using TBHP as terminal oxidant after 2 h

Scheme 2

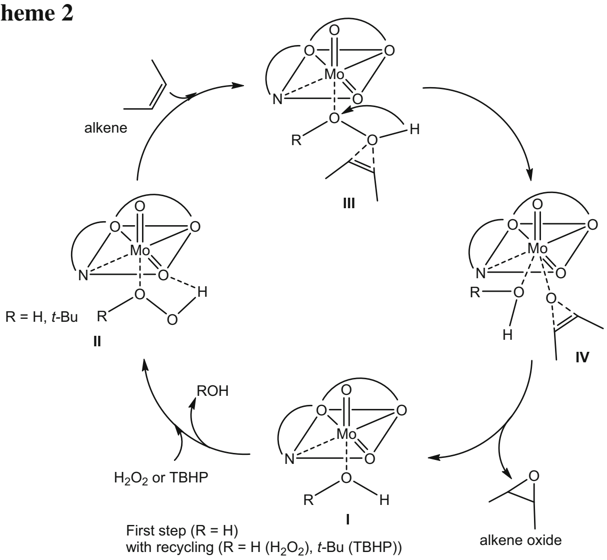

compared to acetonitrile, and its coordination to the metal center is expected to be more facile than with acetonitrile. Accordingly, the lower catalytic activity of the title catalysts **1**, **2**, and **3** in methanol, compared to that in acetonitrile, it seems to be due to the greater competition between the peroxide and the later for occupying the coordination sites to Mo ion (Scheme 2). These results might be confirmed also by the effect of strong coordinatively solvents, i.e. acetone and THF. The conversion percentage of 1,2-cyclooctene using either aqueous H_2O_2 or TBHP reduced significantly in THF (26, 17, and 27 % with aqueous H_2O_2 and 27, 22, and 27 % with TBHP, catalyzed by **1**, **2**, and **3**, respectively) (Table 7). Consequently, the higher chemo- and stereoselective conversion of 1,2-cyclooctene in acetonitrile relative to methanol and THF is due to the high coordination ability of those solvents to the central metal ion.

The solubility of *cis*-MoO_2 complexes **1**, **2**, or **3** [28] may also play an observable role in their catalytic potentials. **1**, **2**, and **3** are sparingly soluble in dichloromethane and chloroform in which the catalytic ability of the current complex catalysts deactivated and exhibited very low yield of the oxidation process heterogeneously, especially with aqueous H_2O_2 (Table 7). In addition, H_2O_2 has a very low miscibility in low dielectric constants, i.e. dichloromethane and chloroform, but is highly miscible in the other polar solvents with highest dielectric constants, i.e. acetonitrile and methanol, as observed by Monfared et al. [54]. This may explain the low chemo- and stereoselective conversion of 1,2-cyclooctene in dichloromethane and chloroform with aqueous H_2O_2 as an oxidant (9, 9, and 4 % in dichloromethane and 16, 13, and 23 % in chloroform, catalyzed by **1**, **2**, and **3**, respectively; Table 7). Moreover, the organic nature of TBHP may elucidate its high oxidizing reactivity in chloroform and dichloromethane catalyzed by **1**, **2**, or **3** to award good selective conversion of 1,2-cyclooctene (45, 46, and 53 % in dichloromethane and 56, 57, and 59 % in chloroform, catalyzed by **1**, **2**, and **3**, respectively).

The consumed long time for the 1,2-cyclooctene oxidation (8 h at 70 °C) with aqueous H_2O_2 in acetonitrile within **1**, **2**, or **3** as a catalyst compared to that with TBHP (2 h at 70 °C) in the same conditions is probably explained by the high amount of water in the reaction media with aqueous H_2O_2. The high amount of water perhaps deactivates the catalytic potentials of the catalyst complexes by a competition through coordination to the unsaturated active site to the central metal ion [55]. Additionally, the organic nature of TBHP may improve the oxidizing reactivity in the organic solvent (acetonitrile) compared to aqueous H_2O_2. In other words, the need to insure the homogeneous conditions of the substrates, 1,2-cyclooctene is usually immiscible within H_2O_2/H_2O in acetonitrile phase [55] which proceeded long time and at high temperature (Table 3). The coordinated water molecules as labile ligands should also be taken into account, which may also play a major role for inhibition of the complexes' catalytic potentials (Scheme 2, I). *cis*-MoO_2 complexes **1**–**3** contain coordinatively unsaturated centers that play a major role of a catalytic redox site [4]. In general, the proposed mechanisms for the oxidation of alkenes with *cis*-MoO_2 complexes involve coordination of the oxidant to the metal center [56, 57] within substitution of the solvent molecule by the oxidant in the catalytic processes [58]. This could be explained by the redshift of the characteristic electronic absorbance band from 381 to 403 nm of complex **2** after the addition of aqueous H_2O_2 to the reaction media (Fig. 2) of the oxidation of 1,2-cyclooctene. The substitution of the coordinated water molecule by H_2O_2 molecule in the oxygenation process caused little shift of the characteristic absorption band in the catalyst complex **2**.

Temperature effect

Attempts were made to investigate the effect of temperature on the rate and control selectivity of the conversion protocol of 1,2-cyclooctene. The reaction carried out in various temperatures at 40, 50, 60, and 70° C catalyzed by **1**. The results are collected and presented in Fig. 3. Figure 3 shows the time-dependent curves of the oxidation reactions employing **1** as catalysts and aqueous H_2O_2 as oxygen donor. The observed kinetic profiles present that the catalytic activity of **1** is performed with increase of the reaction temperature. At low temperatures, 40 and 50 °C, the catalytic potential of **1** was very slow and gave low chemo- and stereoselective conversion after long

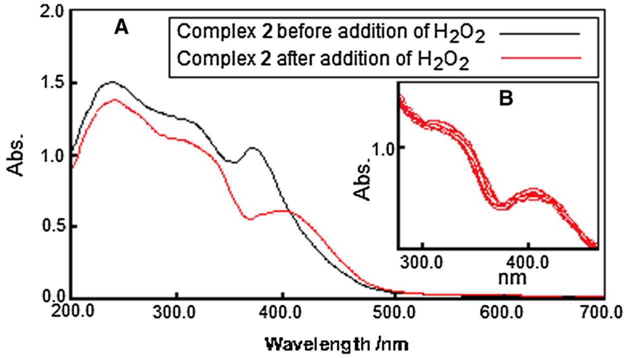

Fig. 2 **a** Electronic spectral scan of complex **2** before and after addition of aqueous H_2O_2 to the reaction media in the presence of 1,2-cyclooctene in acetonitrile at 70 °C. **b** The repeated electronic spectral scan of complex **2** with delay time 1 h

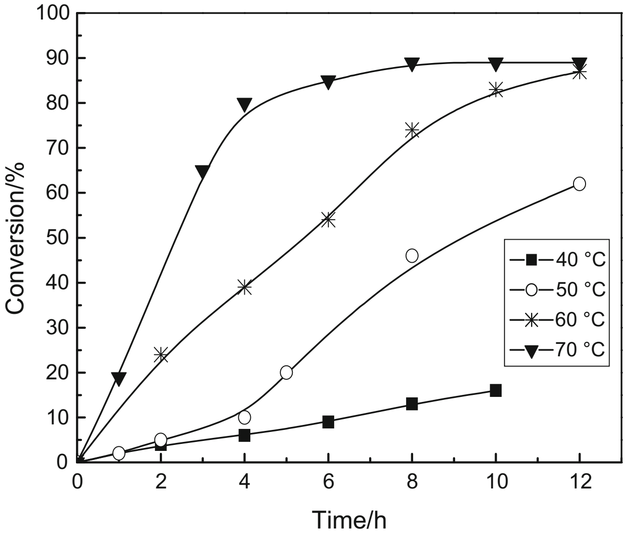

Fig. 3 Kinetic profiles of 1,2-cyclooctene oxidation with aqueous H_2O_2 in acetonitrile in presence of **1** at different temperatures for 12 h

time (16 % after 10 h and 62 % after 12 h, respectively). At high temperatures, 60 and 70 °C, the catalytic process afforded the highest conversions (87 % after 12 h and 89 % after 8 h, respectively), especially at 70 °C which gave an optimal chemo- and stereoselective and controlled yield product of 1,2-epoxycyclooctane-catalyzed complex **1** with aqueous H_2O_2 with shorter time (8 h).

The solubility of the studied complexes may play a major role for their catalytic activity. Complex **1** is not highly active at low temperature probably due to the low solubility of such dihydrazone complexes in acetonitrile converting the catalytic process to be heterogeneous [32–35, 38]. The ability to open a coordination site for the oxidant molecule, by replacing the coordinative solvent molecule (water) with the oxidant molecule may also have responsibility for their catalytic activity, which is not easy to carry out at low temperatures to form activated species. This will be discussed in the mechanistic aspects (Scheme 2, II).

The mechanistic aspects

Various alkenes were subjected to the oxidation protocol under the influence of **1**, **2**, and **3** catalysts, to establish the catalytic applicability of the current complex catalysts. Tables 4 and 5 summarized the oxidation product yield of the some different alkenes by chemo- and stereoselectivity using either aqueous H_2O_2 or TBHP in acetonitrile catalyzed by **1**, **2**, or **3** (entries 1–7) at 70 °C.

Inspections of the results in Tables 4 and 5 indicate several useful features of this catalytic process. The least reactive aliphatic terminal and cyclic alkenes were oxidized in desired times in good/excellent yields and excellent selectivities (Table 4, entries 1–3 with aqueous H_2O_2 and Table 5, entries 1–3 with TBHP) in which the chemo- and stereoselectivity of the procedure was notable and measured by GC. The complete retention of configuration in the oxidation of styrene was obtained in excellent stereoselectivity (Tables 4 and 5, entry 4), whereas the stereoselective conversion of the chain aliphatic alkenes was good/excellent as shown in Tables 4 and 5 (entries 4–6). It took longer time with aqueous H_2O_2 (ca. 10 h) compared with TBHP (ca. 2.5 h).

Due to the structural features of *cis*-MoO_2 unit with *bis*-tridentate Schiff base ligands [4, 13], *cis*-MoO_2 complexes **1**, **2**, and **3** have an open coordination site for the oxidant activation occupied by water molecule (Scheme 2, I) which is useful for catalytic oxidation reactions, replacing of the coordinated water molecule by the oxidant molecule, i.e. H_2O_2 or TBHP (Scheme 2, II). This behavior has been widely reported [4, 49, 50] and proved particularly by the electronic spectral scan of **2** in the reaction media before and after addition of aqueous H_2O_2 (Fig. 2a). The electronic spectral scan of **2** in acetonitrile solution before and after adding aqueous H_2O_2 at 70 °C indicates that the catalyst is stable under the catalysis conditions (Fig. 2a). The above observations are in stark contrast with previous reports, where 1,2-cyclooctene oxidation by Mo^{VI} complexes was described as efficient only for TBHP as an oxidant in non-aqueous media, whereas the presence of water in excess or the use of aqueous H_2O_2 as an oxidant was reported to give rise to catalyst deactivation [13, 46, 47]. The most probability for the stability of Mo ions in the reaction media has elucidated by monitoring the repeated electronic spectral scans of complex in the oxidation process (Fig. 2b). The intensity of the characteristic absorption bands remains approximately unchanged during the reaction time (381 and 403 nm) [13].

The initial decrease in the intensity upon addition of the oxidant may be attributed to the formation of active species in the oxidation reaction (Scheme 2, II) [13, 58, 59]. According to the designed tentative mechanism, the second stage of the process is the interaction between the alkene molecule and the activated H_2O_2 or TBHP molecule in the coordination sphere of the molybdenum complex (Scheme 2, III) [49, 50]. The Lewis acidity of the Mo center increases the oxidizing power of the oxo group and the alkene is subsequently oxygenated by nucleophilic attack on an electrophilic oxygen atom of the coordinated H_2O_2 or TBHP (Scheme 2, III) [53]. The reaction mechanism involves an activation state formed between the complex, oxidant, and alkene (Scheme 2, III) [51, 52], affording an activated structural intermediate of the complex, solvent (water from H_2O_2 or *tert*-butanol from TBHP) and alkene oxide (Scheme 2, IV) [4, 13]. In the catalytic process, in higher conversions, water (from H_2O_2) or *tert*-butanol (*t*-BuOH, from TBHP) probably competes with H_2O_2 or TBHP (Scheme 2, recycling of the catalytic process, I) for coordination to the molybdenum center, forming a less reactive species that leads to the decreasing reaction rate with either H_2O_2 or TBHP, respectively [51].

The impact of the electronic and structural features of the dihydrazone ligands **1**–**3** on the stability and catalytic potential of the Mo catalyst was investigated. Different electronically and structurally Mo complexes were subjected to the oxidation of some various alkenes by either aqueous H_2O_2 or TBHP (Tables 4, 5). The order of catalytic activity was found to be $\mathbf{3} > \mathbf{2} > \mathbf{1}$ according to turnover frequency of the catalysts per hour (Scheme 1). As expected, an electron withdrawing ability of the phenyl ring of the terephthalo group in **3** increases the effectiveness of the catalyst, resulting from the elevated Lewis acidity of the molybdenum center and therefore the activation of aqueous H_2O_2 or TBHP (Scheme 2, III) [59]. The remarkable reductions of the catalytic activity of **1** and **2** compared to **3** may be due to the electron-donating ability of methylene and ethylene groups in **1** and **2**, respectively, which is resulted from the low Lewis acidity of the molybdenum center toward aqueous-H_2O_2 or TBHP.

The performing results for the activity and stability of these easily prepared current complexes during the oxidation reactions (Scheme 2, I), leading to high/excellent conversion at reasonably low reaction times with TBHP, along with excellent chemo- and stereoselectivity conversion are strong advantages of the present *cis*-MoO_2 complexes as oxidation catalysts [4].

Experimental

All reactions were carried out with magnetic stirring and held at the chosen temperature by immersion in a thermostated oil bath. H_2O_2, TBHP, all alkenes, and solvents were used as received from commercial suppliers (Sigma-Aldrich and Acros). The bis-tridentate 2-(*o*-hydroxybenzylidene)dihydrazone ligands **L1**–**L3** were obtained from the common condensation of malonyl [32, 33], succinyl [34, 35], and terephthalo [38] dihydrazide with salicylaldehyde [28] (Supplementary Material). Complexes **1**–**6** are characterized by IR, ^{1}H NMR, ^{13}C NMR, and UV–Vis spectra, thermogravimetric analyses (TGA), and elemental analyses (EA) [26] (Tables 1, 2).

NMR spectra were measured in the Central Lab, Chemistry Department, Faculty of Science, Sohag University at 25 °C on a multinuclear FT-NMR spectrometer Bruker ARX400 at 400.1 (^{1}H) and 100.6 (^{13}C) MHz. The ^{1}H and ^{13}C chemical shifts δ are given in ppm. Coupling constants refer to J_{HH} in ^{1}H and J_{CC} in ^{13}C NMR unless denoted otherwise. Splitting pattern for larger and smaller coupling constants is given in the same order as the J values. Mass spectra were recorded in Central Lab, Assiut University, Jeol JMS600 spectrometer superconducting magnet with EI+. Elemental analyses were carried out with a CHNS-932 analyzer from LECO using standard conditions in Microanalytical Center in Cairo University. The electronic spectra of the current ligands and complexes **1**–**6** were measured using 10 mm silica cells in the thermostatted cell holder of a Jasco UV–Vis spectrophotometer (model V-530). The thermostatted cell holder was supplied by an ultrathermostat water circulator (HAAKE Model F3-k). Thermogravimetric analysis (TGA) was carried out in dynamic nitrogen atmosphere (20 cm^3 min^{-1}) with heating rate 10 °C using Shimadzu TGA-50H thermal analyzer. Melting points were obtained by a Thermo Scientific 9100 apparatus.

General procedure for the synthesis of complexes 1–6

The metal compound (bis(acetylacetonato)dioxomolybdenum(VI) or uranyl acetate) dissolved in 10 cm^3 methanol was added vigorously to a methanolic solution (15 cm^3) of **L1**–**L3** (as suspended solution). The reaction mixture was refluxed under stirring for few hours. The metal complexes were precipitated after cooling then filtrated, washed many times with methanol and diethyl ether, and dried in vacuum. The metal complex was recrystallized in hot solution of methanol–acetonitrile (1:1).

*Bis(2-hydroxy-1-benzylidene)malonyldihydrazone dimolybdenyl·monohydrate (**1**)*

Prepared from 0.10 g **L1** (0.28 mmol) and 0.19 g MoO_2 $(acac)_2$ (0.58 mmol); reflux was for 2 h. Orange solid; m.p.: >300 °C; yield 0.12 g (63 %). The NMR results are in accordance with the reported complex by Zhang et al. [32].

Bis(2-hydroxy-1-benzylidene)succinyldihydrazone dimolybdenyl·monohydrate (**2**)

Prepared from 0.15 g **L2** (0.42 mmol) and 0.27 g $MoO_2(acac)_2$ (0.84 mmol); reflux was for 2 h. Orange solid; m.p.: >300 °C; yield 0.18 g (66 %). The NMR results are in accordance with the reported complex by Ahmed et al. [34].

Bis(2-hydroxy-1-benzylidene)terephthalodihydrazone dimolybdenyl·monohydrate (**3**, $[(MoO_2)_2\mathbf{L3}(H_2O)_2]\cdot H_2O$)

Prepared from 0.15 g **L3** (0.372 mmol) and 0.24 g $MoO_2(acac)_2$ (0.745 mmol); reflux was for 2 h. Orange solid; m.p.: >300 °C; yield 0.10 g (62 %). ^1H NMR (400 MHz, DMSO-d_6): $\delta = 3.89$ (s, H_2O), 6.97 (d, $J = 8.2$ Hz, 2H, ArH), 7.10 (t, $J = 7.3$ Hz, 2H, ArH), 7.56 (t, $J = 7.5$ Hz, 2H, ArH), 7.76 (d, $J = 7.1$ Hz, 2H, ArH), 8.07–8.14 (m, 4H, ArH), 9.00 (s, 2H, CH=N) ppm; ^{13}C NMR (100 MHz, DMSO-d_6): $\delta = 118.0$ (CH), 119.5 (C_q), 121.1 (CH), 127.6 (CH), 127.7 (CH), 129.0 (CH), 131.6 (C_q), 132.5 (C_q), 133.6 (C_q), 133.9 (CH), 134.6 (CH), 156.0 (CH), 156.3 (CH), 158.8 (CH), 165.0 (C_q), 167.1 (C_q) ppm.

Bis(2-hydroxy-1-benzylidene)malonyldihydrazone diuranyl·monohydrate (**4**, $[(UO_2)_2\ \mathbf{L1}(H_2O)_4]\cdot H_2O$)

Prepared from 0.10 g **L1** (0.28 mmol) and 0.24 g $UO_2(OAc)_2\cdot 2H_2O$ (0.58 mmol); reflux was for 1 h. Brownish red solid; m.p.: >300 °C; yield 0.22 g (80 %). ^1H NMR (400 MHz, DMSO-d_6): $\delta = 3.35$ (s, H_2O), 3.87 (s, CH_2), 6.70 (d, $J = 4.4$ Hz, 2H, ArH), 6.93 (s, 2H, ArH), 7.46 (d, $J = 4.7$ Hz, 2H, ArH), 7.53 (s, 2H, ArH), 9.19 (s, 2H, CH=N) ppm; ^{13}C NMR (100 MHz, DMSO-d_6): $\delta = 40.9$ (CH_2), 115.7 (CH), 119.2 (C_q), 122.8 (CH), 132.3 (CH), 133.0 (CH), 156.5 (CH), 167.4 (C_q), 174.4 (C_q) ppm.

Bis(2-hydroxy-1-benzylidene)succinyldihydrazone diuranyl (**5**, $[(UO_2)_2\ \mathbf{L2}(H_2O)_4]$)

Prepared from 0.10 g **L2** (0.28 mmol) and 0.23 g $UO_2(OAc)_2\cdot 2H_2O$ (0.56 mmol); reflux was for 1 h. Brownish red solid; m.p.: >300 °C; yield 0.19 g (71 %). ^1H NMR (400 MHz, DMSO-d_6): $\delta = 3.15$ (s, 4H, CH_2), 3.37 (s, H_2O), 6.68 (t, $J = 7.3$ Hz, 2H, ArH), 6.94 (d, $J = 8.1$ Hz, 2H, ArH), 7.46 (t, $J = 7.7$ Hz, 2H, ArH), 7.51 (d, $J = 7.3$ Hz, 2H, ArH), 9.14 (s, 2H, CH=N) ppm; ^{13}C NMR (100 MHz, DMSO-d_6): $\delta = 31.2$ (CH_2), 115.8 (CH), 119.1 (CH), 122.9 (C_q), 132.3 (CH), 132.9 (CH), 156.4 (CH), 167.3 (C_q), 177.1 (C_q) ppm.

Bis(2-hydroxy-1-benzylidene)terephthalodihydrazone diuranyl (**6**, $[(UO_2)_2\ \mathbf{L3}(H_2O)_4]$)

Prepared from 0.12 g **L3** (0.298 mmol) and 0.25 g $UO_2(OAc)_2\cdot 2H_2O$ (0.596 mmol); reflux was for 1 h. Pale orange solid; m.p.: >300 °C; yield 0.20 g (69 %). ^1H NMR (400 MHz, DMSO-d_6): $\delta = 3.91$ (s, H_2O), 6.73 (dd, $J = 6.4$ Hz, 2H, ArH), 6.68 (t, $J = 7.1$ Hz, 2H, ArH), 7.51 (t, $J = 7.4$ Hz, 2H, ArH), 7.60 (d, $J = 6.1$ Hz, 2H, ArH), 8.14 (d, $J = 8.0$ Hz, 2H, ArH), 8.51 (d, $J = 8.0$ Hz, 2H, ArH), 8.55 (s, 2H), 9.32 (d, $J = 4.4$ Hz, 2H, CH=N) ppm; ^{13}C NMR (100 MHz, DMSO-d_6): $\delta = 115.9$ (CH), 116.0 (CH), 119.3 (C_q), 122.8 (CH), 123.0 (CH), 127.5 (CH), 127.7 (CH), 128.6 (CH), 130.1 (C_q), 132.6 (CH), 132.8 (CH), 133.2 (CH), 133.3 (CH), 136.8 (C_q), 139.9 (C_q), 157.8 (CH), 158.6 (CH), 165.4 (C_q), 167.5 (CH), 167.6 (CH), 170.0 (C_q), 170.9 (C_q) ppm.

Catalytic procedure

1,2-Cyclooctene (0.13 cm^3, 1.0 mmol) or other alkene (1.0 mmol) was added to a solution of **1–6** contacted to air (0.01, 0.02, or 0.04 mmol) in 10 cm^3 of acetonitrile (or other solvents) at 40, 50, 60, or 70 °C in an oil bath under magnetic stirring. The reaction was initiated by charging with either 0.5 cm^3 aqueous H_2O_2 (30 %, 4.16 mmol) or 0.2 cm^3 TBHP (70 % in water, 2.0 mmol) at the typical temperature. The reaction was monitored by gas chromatographic analyses, using computerized standard calibration curve. The oxidation products were identified by comparing their retention times with those of authentic samples. Control reactions were carried out by withdrawing samples (ca. 2 cm^3) of the reaction mixture and treatment of the reaction mixture with MnO_2 to quench the excess aqueous H_2O_2 or TBHP and with anhydrous sodium sulfate, under the same conditions in the catalytic runs. The resulting slurry was filtered on Celite, and the filtrate was injected in the GC. This allowed independent measurements for each sample. The conversion of 1,2-cyclooctene to 1,2-epoxycyclooctene was calculated according to computerized standard calibration curves.

Gas chromatography is computerized Agelient 5890A 1909 J-413: 325 °C equipped with a flame ionization detector and a HP-5 capillary column (phenyl methyl siloxane 30 m × 320 μm × 0.25 μm). All the reactions were run at least in duplicate.

References

1. Sheldon RA, Kochi JK (1981) Metal-catalysed oxidations of organic compounds. Academic Press, New York
2. Franz G, Sheldon RA (1991) In: Elvers B, Hawkins S, Shulz G (eds) UIlmann's Encyclopedia of Industrial Chemistry, vol A18, 5th edn. VCH, Weinheim, p 261
3. Lutz JT (1980) In: Grayson M, Eckroth D, Bushey GJ, Eastman CI, Klingsberg A, Spiro L (eds) Kirk-Othmer Encyclopedia of Chemical Technology, vol 9, 3rd edn. Wiley, New York, p 251
4. Bagherzadeh M, Zare M, Amani V, Ellern A, Woo LK (2013) Polyhedron 53:223
5. Rayati S, Zakavi S, Koliaei M, Wojtczak A, Kozakiewicz A (2010) Inorg Chem Commun 13:203
6. Rayati S, Ghasemi A, Sadeghzadeh N (2010) Catal Commun 11:792

7. Zakavi S, Ashtiani AS, Rayati S (2010) Polyhedron 29:1492
8. Zakavi S, Heidarizadi F, Rayati S (2011) Inorg Chem Commun 14:1010
9. Brito JA, Ladeira S, Teuma E, Royo B, Gomez M (2011) Appl Catal A Gen 398:88
10. Neves P, Amarante TR, Gomes AC, Coelho AC, Gago S, Pillinger M, Gonçalves IS, Silva CM, Valente AA (2011) Appl Catal A Gen 395:71
11. Hu Z, Fu H, Li Y (2011) Inorg Chem Commun 14:497
12. Ln Y, Fu X, Gong B, You X, Tu X, Chen J (2010) J Mol Catal A Chem 322:55
13. Rezaeifard A, Sheikhshoaie I, Monadi N, Alipour M (2010) Polyhedron 29:2703
14. Mimoun H, Seree de Roch I, Sajus L (1970) Tetrahedron 26:37
15. Sharpless KB, Townsend JM, Williams DR (1972) J Am Chem Soc 94:295
16. Romao MJ, Archer M, Moura I, Moura JJG, LeGall J, Engh R, Schneider M, Hof P, Huber R (1995) Science 270:1170
17. Kramer SP, Johnson JL, Ribiero AA, Millington DS, Rajagopalan KV (1987) J Biol Chem 262:16357
18. Lane BS, Burguess K (2003) Chem Rev 103:2457
19. Grigoropoulos G, Clark JH, Elings JA (2003) Green Chem 5:1
20. Tang MC-Y, Wong K-Y, Chan TH (2005) Chem Commun 10:1345
21. Maiti SK, Banerjee S, Mukherjee AK, Abdul Malik KM, Bhattacharyya R (2005) New J Chem 29:554
22. Mitchell JM, Finney NS (2001) J Am Chem Soc 123:862
23. Belgacem J, Kress J, Osborn JA (1992) J Am Chem Soc 114:1501
24. Jain KR, Herrmann WA, Kühn FE (2008) Coord Chem Rev 252:556
25. Sobczak JM, Ziołkowski J (2003) J Appl Catal A 248:261
26. Zhao J, Zhou X, Santos AM, Herdtweck E, Romäo CC, Kühn FE (2003) J Chem Soc Dalton Trans (19):3736
27. Sessler JL, Melfi PJ, Dan Pantos G (2006) Coord Chem Rev 250:816
28. Adam MSS, Sulamain MGM, Abdelkareem AAM (2014) Int J Chem 35:1410
29. Fortier S, Hayton TW (2010) Coord Chem Rev 254:197
30. Bernhardt PV, Chin P, Sharpe PC, Richardson DR (2007) J Chem Soc Dalton Trans 30:3232
31. Melnyk P, Leroux V, Sergheraerta C, Grellier P (2006) Bioorg Med Chem Lett 16:31
32. Zhang C, Rheinwald G, Lozan V, Wu B, Lassahn P-G, Lang H, Janiak C (2002) Z Anorg Allg Chem 628:1259
33. Lal RA, Choudhury S, Ahmed A, Borthakur R, Asthana M, Kumar A (2010) Spectrochim Acta A 75:212
34. Ahmed A, Chanu OB, Koch A, Lal RA (2012) J Mol Struct 1029:161
35. Lal RA, Chakrabarty M, Choudhury S, Ahmed A, Borthakur R, Kumar A (2010) J Coord Chem 63:163
36. Nemykin VN, Basu P (2005) Inorg Chem 44:7494
37. Javadi MM, Moghadam M, Mohammadpoor-Baltork I, Tangestaninejad S, Mirkhani V, Kargar H, Tahir MN (2014) Polyhedron 72:19
38. Yin H-D, Cui J-C, Qiao Y-L (2008) Polyhedron 27:2157
39. Orpen AG, Brammer L, Allen FH, Kennard O, Watson DG, Taylor R (1989) J Chem Soc Dalton Trans S1
40. Black DF, de Oliveira GM, Roman D, Ballin MA, Kober R, Piquini C (2014) Inorg Chim Acta 214:6
41. Taylor SH, O'Leary SR (2000) Appl Catal B 25:137
42. Zhang ZT, Konduru M, Dai S, Overbury SH (2002) Chem Commun (20):2406
43. Kumar D, Bhat RP, Samant SD, Gupta NM (2005) Catal Commun 6:627
44. Asadi Z, Zeinali A, Dusek M, Eigner V (2014) Int J Chem Kinet 46(12):718
45. Azam M, Al-Resayes SI, Velmurugan G, Venuvanalingam P, Wagler J, Kroke E (2015) Dalton Trans 44:568
46. Martins AM, Romao CC, Abrantes M, Azevedo MC, Cui J, Dias AR, Duarte MT, Lemos MA, Lourenco T, Poli R (2005) Organometallics 24:2582
47. Kühn FE, Santos AM, Herrmann WA (2005) Dalton Trans 2483
48. Kühn FE, Santos AM, Abrantes M (2006) Chem Rev 106:2455
49. Madeira F, Barroso S, Namorado S, Reis PM, Royo B, Martins AM (2012) Inorg Chim Acta 383:152
50. Mardani HR, Golchoubian H (2006) Tetrahedron Lett 47:2349
51. Grivani G, Tahmasebi V, Khalaji AD, Fejfarova K, Dušek M (2013) Polyhedron 51:54
52. Rayati S, Koliaei M, Ashouri F, Mohebbi S, Wojtczak A, Kozakiewicz A (2008) Appl Catal A Gen 346:65
53. Grivani G, Bruno G, Rudbari HA, Khalaji AD, Pourteimouri P (2012) Inorg Chem Commun 18:15
54. Monfared HH, Bikas R, Mayer P (2010) Inorg Chim Acta 363:2574
55. Dinoi C, Ciclosi M, Manoury E, Maron L, Perrin L, Poli R (2010) Chem Eur J 16:9572
56. Bagherzadeh M, Latifi R, Tahsini L, Amani V, Ellerm A, Woo LK (2009) Polyhedron 28:2517
57. Bibal C, Daran J-C, Deroover S, Poli R (2010) Polyhedron 29:639
58. Rao SN, Kathale N, Rao NN, Munshi KN (2007) Inorg Chim Acta 360:4010
59. Sui Y, Zeng X, Fang X, Fu X, Xiao Y, Chen L, Li M, Cheng S (2007) J Mol Catal A Chem 270:61